Applied Catalysis A: General 383 (2010) 24–32

Contents lists available at ScienceDirect

Applied Catalysis A: General

journal homepage: www.elsevier.com/locate/apcata

Thin layer of carbon-nano-fibers (CNFs) as catalyst support for fast mass transfer in hydrogenation of nitrite

Jitendra Kumar Chinthaginjala [a], Johannes Hendrik Bitter [b], Leon Lefferts [a,*]

[a] Catalytic Processes and Materials, IMPACT and MESA+, University of Twente, PO Box 217, 7500 AE, Enschede, The Netherlands
[b] Inorganic Chemistry and Catalysis Group, Department of Chemistry, Faculty of Sciences, Utrecht University, Sorbonnelaan 16, 3584 CA Utrecht, The Netherlands

ARTICLE INFO

Article history:
Received 27 January 2010
Received in revised form 28 April 2010
Accepted 12 May 2010
Available online 20 May 2010

Keywords:
Carbon-nano-fibers
Nitrite reduction
Structured catalysts

ABSTRACT

CNF-foam 'hairy foam' and CNF aggregates supported Pd catalysts were studied for the reduction of aqueous nitrite solution and also compared with conventional catalysts. Relatively large Pd particle size and similar Pd particle size distribution on all the catalyst supports excludes any structure sensitive effects on reaction. Intrinsic rates over hairy foam catalysts were independent of CNF-layer thickness (8–28 μm) and Pd loading (0.5–2 wt%), demonstrating the absence of any mass transfer limitations. When compared to conventional catalysts at comparable diffusion layers, CNF based catalysts showed at least three times higher rates of nitrite conversion per mole of surface palladium (TOF). Increased TOF is due to the improved mass transfer provided by macroporous structure of the entangled CNFs, which offers low tortuosity, provides accessibility to all the active sites. The intrinsic activity of graphite and CNF-supported Pd contributes significantly to the high activity for nitrite reduction.

1. Introduction

Multiphase reactors are commonly used in many chemical processes aiming to provide good contact between gas and/or liquid reactants with solid heterogeneous catalysts. Conventional technologies for such heterogeneous catalytic reactions comprise slurry reactors and trickle bed reactors. In slurry phase reactors, very small catalyst particles (typically <50 μm) are used providing short diffusion path within the catalyst preventing, or limiting internal mass transfer limitation. However, additional cost for catalyst separation and loss of active metal phase from the catalyst due to attrition are drawbacks, whereas filtration units cause relatively frequent process disturbances [1]. In trickle bed reactors, relatively large catalyst particles sizes (>1 mm) are necessary to limit the pressure drop over the fixed bed. Large catalyst particles induce long diffusion paths within the catalyst particle, thus limiting the mass transfer rate [2]. Presence of concentration gradients within the catalyst decreases overall conversion and induces loss of selectivity.

An interesting proposition is to develop a structured catalyst combining the advantages of slurry phase operation and fixed bed operation. The structured catalyst should provide a large liquid–solid surface area and short diffusion paths within the catalyst, at the same time avoiding the necessity of filtration of small catalyst particles. The application of monoliths, e.g. operated in the Taylor flow regime has been studied extensively [3,4]. Other structural packing including foams [5–8], filters [9], fibers [10,11] and cloths [12] have been explored as well.

Solid foam is an alternative option as a structured packing to improve gas–liquid mass transfer and optimize hydrodynamics [13]. However, the external surface area is by far not sufficient for a catalyst support and a porous layer needs to be added, similar as in the case of monoliths. This layer should be mechanically stable as well as highly porous, maximizing the mass transfer rate which is particularly important for heterogeneous catalytic reactions in liquid phase. Carbon-nano-fibers (CNFs) are mechanically strong, chemically inert and the surface chemistry can be modified [15,16,49], well suited for catalyst support. A general introduction to CNFs relevant to the field of catalysis can be found in the reviews by De Jong and Geus, and Rodriguez [15,18], respectively. Previous work in our group [6,14] demonstrated that extremely porous layers of (CNFs) can be prepared on cylindrical pieces of polycrystalline Ni foam (Fig. 1), which is designated as 'hairy foam', resulting in well attached thin layers with very high porosity and low tortuosity. The open structure of CNFs mimics the inverse structure of conventional porous support material, as suggested by Chinthaginjala et al. [17] and Wenmakers et al. [8]. Good attachment of CNFs to the host support is obviously essential to for any practical application. In the case of hairy foams, CNFs are strongly attached to the Ni foam surface *via* a microporous carbon layer, named C-layer hereafter (Fig. 2), and the roots of the CNFs are embedded in this C-layer. Good interconnections

* Corresponding author. Tel.: +31 53 489 2858/3033; fax: +31 53 489 4683.
E-mail addresses: l.lefferts@utwente.nl, l.lefferts@tnw.utwente.nl (L. Lefferts).

0926-860X/$ – see front matter © 2010 Elsevier B.V. All rights reserved.
doi:10.1016/j.apcata.2010.05.013

Nomenclature

Φ_R	radius of catalyst support, μm
Φ_p	Pd particle size, nm

between Ni surface, C-layer and CNFs induce mechanical stability [14].

This work aims at demonstrating the superior properties of hairy foam over traditional support materials, by using hydrogenation of nitrite in water as an extremely fast model reaction. Hörold et al. [19,20] reported that several noble metals (Pd, Pt, Ru, Ir, Rh) are capable of catalyzing nitrite hydrogenation, Pd being the most active metal. It is reported that hydrogenation of nitrite is extremely fast, easily inducing internal concentration gradients due to diffusion limitation [19,21–23]. Both nitrogen and ammonia are formed in nitrite hydrogenation, according Eqs. (1) and (2) [19,20,24]. It should be noted that not only hydrogen and nitrite are reacting, but also protons are consumed and it is suggested that at neutral pH proton diffusion may be the most limiting factor, causing a pH gradient in the catalyst particles, influencing the selectivity [23]. Strukul et al. [25] reported that ammonia formation is enhanced when using large catalyst particles (>0.5 mm). This was attributed to increased pH values in the centre of the catalyst particles, slowing down the formation of nitrogen more significantly then the formation of ammonia, according kinetic data [20,24].

$$2NO_2^- + 3H_2 + 2H^+ \rightarrow N_2 + 4H_2O \quad (1)$$

$$NO_2^- + 3H_2 + 2H^+ \rightarrow NH_4^+ + 2H_2O \quad (2)$$

Catalytic hydrogenation of nitrite is relevant for nitrite and nitrate removal from drinking water [26], as well as for hydroxylamine synthesis via hydrogenation of nitrite, which is an important industrial intermediate for the synthesis of amines [27]. It is well known that hydrogenation of nitrate proceeds *via* nitrite as an intermediate product and that the hydrogenation of nitrite is faster as compared to nitrate.

Aim of this work is to evaluate the performance of hairy foam as catalyst support for efficient internal mass transfer in a fast liquid phase catalytic reaction. The performance of well-characterized Pd catalysts on CNFs will be compared with the performance Pd catalysts supported on traditional support materials.

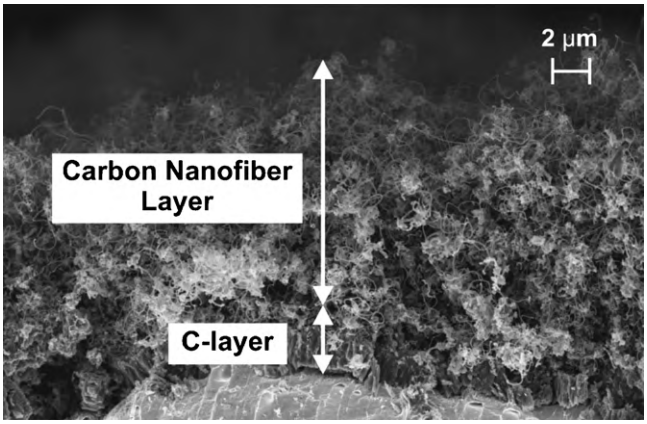

Fig. 2. SEM image of CNF and C-layer on the Ni surface of foam [14].

2. Experimental

2.1. Material

Nitrogen (99.999%, INDUGAS) and ethylene (99.95%, PRAXAIR) were used for CNFs formation without further purification. Hairy foams were prepared by growing CNFs on Ni foam at 440 °C by using 25% ethylene in nitrogen as described in detail previously [14] and the CNFs were not further pre-treated. It was shown previously [28] that we are able to manipulate the thicknesses of both the C-layer as well as the CNF-layer by varying feed composition and time, which was applied to vary the thickness of the CNF-layer in the present study. Table 1 shows the properties of the materials used.

Alumina (AKZO NOBEL), activated carbon (Norit ROX0.8), graphite (EVONIK industries) and silica (AKZO NOBEL) were used as conventional catalyst supports. Palladium acetylacetonate (Alfa Aesar) and toluene (>99.9%, Merck) were used in the preparation of palladium catalysts. Sodium nitrite (>99%, Merck) was used to prepare nitrite solutions for the catalytic experiments.

2.2. Catalyst preparation

2.2.1. Hairy foam catalysts

Organic phase wet impregnation method was used to deposit active metal on the surface of the CNFs in hairy foams. Pd metal

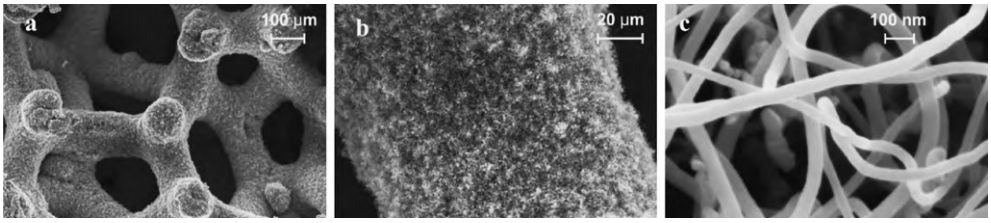

Fig. 1. (a) Overview of the Ni foam after the growth of CNFs at 440 °C in 25% C_2H_4/N_2 for 60 min, (b) CNF coverage on a single strand of the foam, (c) CNFs grown on Ni foam showing macro-void spacing between entangled CNFs [14].

Table 1
Properties of the carbon deposits in the hairy foams used in this study.

	Time of growth (min)	Average CNF-layer thickness (μm)	Average C-layer thickness (μm)	Weight % carbon	BET surface area of Hairy foam (m^2/g)	BET surface area of carbon (m^2/g)
1	25	8	1.5	11.2	10.2	91.1
2	35	13	3	18.1	17.4	96.1
3	60	28	4	29.5	27.7	93.9

Table 2
Palladium dispersion and average Pd particle sizes based on CO-chemisorption on various conventional catalysts and CNF aggregates. The pore volume was determined from desorption isotherm by applying BJH method.

Support type and average particle radius (Φ_R)	Reduction temperatures, °C	Pd, wt%	Pd dispersion, %	Φ_p, nm	Pore volume, ml/g	Tortuosity
Pd/Al_2O_3 (Φ_R: 225 μm)	800	1.64	11.5 ± 0.5	9	0.6	3 [47]
Pd/Al_2O_3 (Φ_R: 21 μm)	800	2.23	11.95 ± 0.2	9	0.6	3 [47]
Pd-silica (Φ_R: 56 μm)	800	2.33	6.5 ± 0.5	17	1.26	3
Pd-activated carbon (Φ_R: 225 μm)	400	1.62	7.8 ± 0.8	14	0.197	4 [48]
Pd-activated carbon (Φ_R: 21 μm)	250	2.33	8.3 ± 0.8	13	0.197	4 [48]
Pd-graphite (Φ_R: 56 μm)	430	2.37	12.4 ± 0.3	9	0.38	4
Pd-unsupported CNF aggregates (Φ_R: 225 μm)	250	1.21	5.3 ± 0.1	21	–	–
Pd-unsupported CNF aggregates (Φ_R: 21 μm)	250	1.48	5.5 ± 0.1	20	–	–

particles were prepared by using palladium acetylacetonate dissolved in toluene. Hairy foam supports were immersed in 40 ml toluene, containing the proper amount of Pd precursor dissolved, in a round bottomed flask of a vacuum rotary evaporator. The flask was immersed in silicon oil bath maintained at a temperature of 50 °C. Toluene was completely evaporated by slowly applying vacuum and leaving behind the palladium precursor deposited on the hairy foam. The Pd loading is always expressed per gram CNF.

2.2.2. Conventional catalysts

Alumina and activated carbon with two different particle sizes were used, ranging between 300–600 μm and 38–45 μm respectively. Graphite and silica catalyst supports were used with a single particle size, ranging between 100 μm and 125 μm. Palladium precursor was deposited *via* organic phase wet impregnation method, applying similar catalyst preparation conditions as used for preparing hairy foam supported catalysts.

Unsupported CNF aggregate catalysts were received from Utrecht University, which were prepared as described by Van der Lee et al. [29]. Two sets of particle sizes ranging between 300–600 μm and 38–45 μm were prepared *via* mortaring and sieving. CNF aggregates were loaded with palladium following the same preparation methods as described above. From here on the packed bed support particle sizes are referred in average particle radius.

CNF-supported catalysts were calcined at 250 °C (ramp of 5 °C/min) during 1 h and then reduced at same temperature during 2 h. The samples were cooled down to room temperature in nitrogen at a ramp of 10 °C/min. Catalysts on conventional supports were also calcined at 250 °C (ramp of 5 °C/min) during 1 h, where after the reduction temperature was varied in order to obtain similar palladium dispersions for all the catalysts in this study; calcination temperatures applied are presented in Table 2.

2.3. Catalytic hydrogenation of nitrite

Catalytic hydrogenation of nitrite was performed in a fixed bed reactor placed in an oven at 298 K. Nitrite concentration in the aqueous reactant solution was always maintained at ~20 mg/l (435 μmol/l) and the pH of the solution was maintained at 7. The solution was pre-saturated at a hydrogen partial pressure of 0.4 bar (balance argon), resulting in a concentration of dissolved H_2 equal to 312 μmol/l, based on Henry's coefficient [30]. The reactor bed volume was varied between 0.29 cm^3 and 1.74 cm^3. The reactor was made of PEEK (polyether–ether–ketone) and the diameter was optimized in order to exactly fit with the size of the cylinder shaped pieces (diameter 4.5 mm) of hairy foam catalysts. The total amount of Pd catalyst used was varied between 0.13 μmol and 0.78 μmol when varying bed volume or Pd loading. Liquid containing nitrite and dissolved hydrogen was pumped through the fixed bed reactor with flowrates up to 12 ml/min with an HPLC pump (DIONEX, Ultimate 3000). The pressure drop induced was less than 0.3 bar in case of hairy foam and varying between 0.8 bar and 4 bar for packed bed catalysts. The space velocity was calculated based on the total volume of the catalyst bed in the reactor chamber. Nitrite and ammonium concentrations in the reactants and products were measured with ion chromatography (DIONEX, ICS 1000).

The reaction was performed under differential conditions, maintaining the nitrite conversions at ~5% in most cases, increasing to maximal 12% occasionally. Therefore, concentration gradients along the axis of the reactor are not significant and turn over frequencies (activity per active site per second, TOF) can be calculated directly from the data by using the Pd dispersion of the relevant catalyst. Packed beds were reproducible for all the catalysts eliminating any tunnelling effect along the bed and measures were taken to precisely fit the hairy foams in the reactor chamber avoiding any bypassing of the liquid flow.

All Pd catalysts were used for typically 16 h and occasionally samples were up to 30 h on stream. In all experiments no significant deactivation was observed and any variation with time-on-stream is included in the error margins indicated in the results.

2.4. Characterization

BET surface area of CNFs was calculated from the N_2-adsorption isotherm obtained at 77 K (Micromeritics Tristar). X-ray fluorescence spectroscopy (XRF) was used to determine the palladium loading on γ-alumina, activated carbon, silica, graphite and CNF aggregates. Inductively coupled plasma (ICP) was used to determine the palladium loadings on hairy foam. CO-chemisorption (Micromeritics, ChemiSorb 2750: Pulse Chemisorption system) at room temperature was used to determine the dispersion of palladium. The palladium particle size distribution was determined for selected catalysts with Transmission Electron Microscopy (TEM—Philips CM300ST-FEG). Thirty-five TEM images were obtained on each catalyst accounting at least 300 Pd particles. The averaged crystal size of palladium particles was determined with line-broadening analysis in X-ray diffraction (XRD), according the Scherrer equation. XRD was performed using a PANalytical X'pert-APD powder diffractometer equipped with a position sensitive detector analyzed over the 2θ-range 15–90° using Cu Kα1 (λ = 1.78897 Å) radiation. Scanning Electron Microscopy (LEO 1550 FEG-SEM) equipped with energy dispersive X-ray analysis (EDX; Thermo Noran Vantage system) was used to qualitatively study the distributions of Pd through cross-sections of the CNF and C-layers in hairy foam catalyst, as well as through cross-sections of the alumina support. Cross-sections of hairy foams were simply obtained by cutting with scissors resulting in well-maintained CNF-layers, allowing analysis with EDX at discrete spots. The alumina support was embedded in a polymer before preparing a cross-section with a microtome. The polymer embedded alumina catalyst particles result in flat cross-sections after dissection, enabling SEM-EDX mapping.

Table 3
Palladium metal dispersions and average Pd particle size based on CO-chemisorption on various hairy foam samples.

Support type	wt%	Dispersion	Φ_p, nm
Hairy foam CNFthickness: 28_{avg} μm	2.23	5.6 ± 0.4	20
	1.97	6.7 ± 0.3	16
Hairy foam CNFthickness: 13_{avg} μm	1.52	9.6 ± 0.2	12
	1.1	9.6 ± 0.3	12
Hairy foam CNF thickness: 8_{avg} μm	0.49	6.7 ± 0.4	16
	1.95	5.4 ± 0.2	20

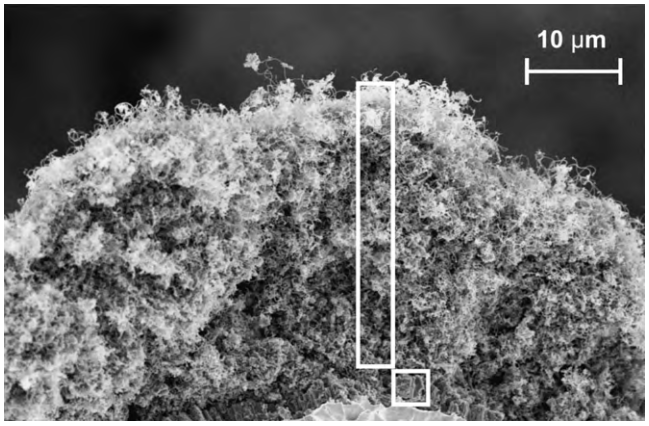

Fig. 3. The cross-section of the hairy foam strand with a homogenous coverage of a 28 μm CNF-layer and 4 μm C-layer. The SEM image is an illustration upon which areas (marked) were selected to analyze Pd concentration by SEM-EDX.

3. Results

3.1. Characterization

3.1.1. Characterization of Pd on hairy foam

Hairy foam samples with different CNF-layer thicknesses were loaded with approximately 2 wt% palladium. Samples with Pd loadings between 0.5 wt% and 2 wt%,were prepared on hairy foam with a 13 μm thick CNF-layer. Table 3 presents the resulting Pd loadings as well as palladium dispersions, as determined with CO-chemisorption. In all cases the Pd dispersion is below 10% and the average Pd particle size is larger than 10 nm. Average Pd particle size was estimated assuming hemispherical shaped particles.

The distribution of Pd within the CNF-layer and C-layer was qualitatively measured with SEM-EDX. Fig. 3 shows a typical cross-sectional view of one of the strands, containing a C-layer on the Ni surface with the CNF-layer on top. EDX was performed at five different spots (3 × 3 μ) at the cross-section of the CNF-layer and one spot in the C-layer. Five different strands were analyzed and the ratio of palladium to carbon is presented as function of the position in Fig. 4. The palladium concentration is significantly higher in the outer 10 μ of the CNF-layer as compared to the deeper CNF-layer as well as the C-layer.

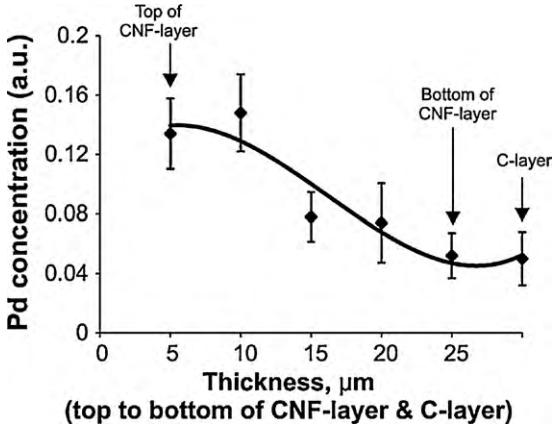

Fig. 4. Qualitative results of Pd distribution across a 28_{avg} μm thick CNF-layer of 2.23 wt% Pd on hairy foam.

3.1.2. Characterization of Pd on alumina support

Palladium dispersions as well as estimated average particle size according to CO-chemisorption on conventional catalyst supports after reduction at indicated temperatures are presented in Table 2. In all cases, the Pd dispersion was less than 13% and the average Pd particle size was at least 8 nm. The distribution of palladium through γ-alumina (225_{avg} μm) was studied by SEM-EDX mapping. Fig. 5a shows a typical SEM image of the cross-section of a particle of a γ-alumina supported palladium catalyst; SEM-EDX mapping in Fig. 5b reveals that Pd is homogeneously distributed in the alumina particle.

Transmission electron microscopy was used to determine the size distribution of palladium particles on alumina, activated carbon and hairy foam catalysts, resulting in Pd particle size distributions as presented in Fig. 6. The Pd particle size distributions are quite similar on all the supports. The averaged Pd particle size based on TEM analysis is presented in Table 4, along with XRD-LB analysis of the same catalysts are presented in Table 4, resulting in similar numbers. Differences with CO-chemisorption data will be discussed later.

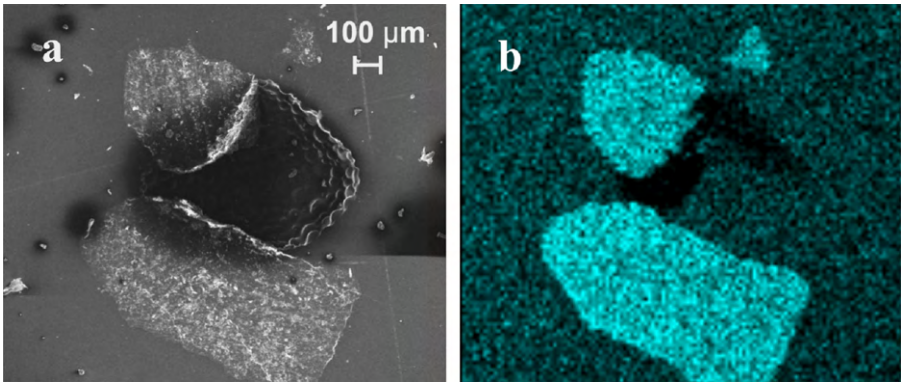

Fig. 5. (a) SEM image of a 1.64 wt% Pd on γ-alumina catalyst of particle radius 225_{avg} μm. (b) shows the mapping images of Pd as analyzed by SEM-EDX.

Table 4
Mean crystal size of palladium on alumina, activated carbon and hairy foams as characterized by CO-chemisorption, transmission electron microscopy and X-ray diffraction line-broadening.

Characterization technique	Mean palladium particle size, nm		
	γ-Alumina (2.23 wt% Pd)	Activated carbon (2.33 wt% Pd)	Hairy foam (2.23 wt% Pd)
[a]CO-chemisorption	13	10	18
TEM	6	5	8
XRD	4.7	4.7	8.7

[a]Selected chemisorption results are a repeat from Tables 2 and 3.

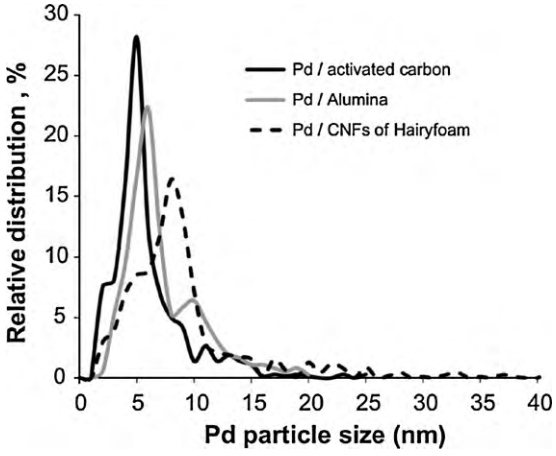

Fig. 6. Palladium particle size distribution on 21 μm particle radius of 2.33 wt% Pd on activated carbon and 2.23 wt% Pd on γ-alumina, and 28 μm CNF-layer of 2.23 wt% Pd on hairy foam catalysts as characterized by TEM.

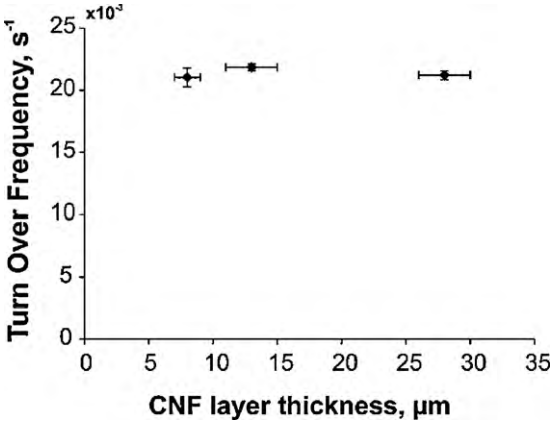

Fig. 8. Rate of nitrite conversion per mole of surface palladium on hairy foam catalysts with CNF-layer thickness between 8 μm and 28 μm and loading of ~2 wt% measured at linear velocity of 55 cm/min and space velocities of 20.2, 33.5 and 50.3 min^{-1} for 8, 13 and 28 $_{avg}$μm, respectively.

3.2. Catalytic tests

3.2.1. Hairy foam catalysts

Nitrite conversion was measured at fixed space time, increasing the linear velocity (*F*, defined as the liquid velocity in an empty reactor) of the reactant stream and increasing the amount of catalyst (W) proportionally, maintaining a space velocity of 25.2 min^{-1}. Fig. 7 shows the nitrite conversion as a function of the linear velocity of the reactant. Nitrite conversion increases with linear velocity below 55 cm/min. In contrast, nitrite conversion is constant at higher velocity, indicating the absence of external mass transfer limitations for linear velocities over 55 cm/min. Therefore, further catalytic experiments with hairy foam catalysts were performed using linear velocity of 55 cm/min.

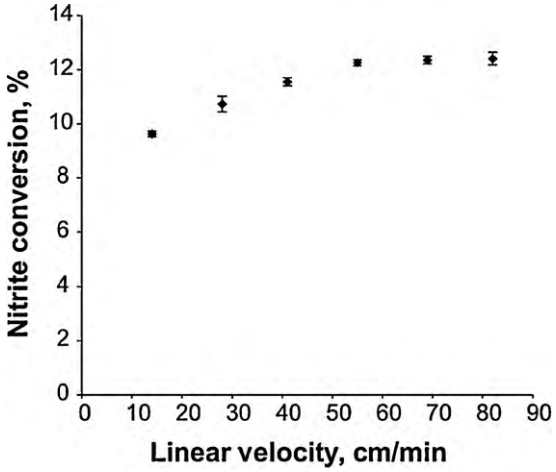

Fig. 7. Nitrite conversion at fixed space time on a 28 μm CNF-layer of 2.23 wt% Pd on hairy foam catalyst at a space velocity of 25.2 min^{-1}.

Fig. 8 shows that the TOF remains constant when the thickness of CNF-layer is varied. The Pd loading was kept constant in this experiment at 2 wt% relative to the carbon loading, implying that the total amount of Pd varies with the CNF-layer thickness. This agrees well with the result in Fig. 9, showing that the TOF does not change when varying the Pd loading on hairy foam with a 13 μ thick CNF-layer. These results clearly demonstrate that both external and internal mass transfer limitations can be excluded, resulting in a TOF equal to 0.021 s^{-1} under the conditions in this study.

3.2.2. Conventional catalysts

Nitrite conversion over Pd on activated carbon (Φ_R: 225 μm) was measured as function of linear velocity, keeping the space velocity constant at 31.5 min^{-1}. Fig. 10 shows that the nitrite conversion increases with the linear velocity below 25 cm/min,

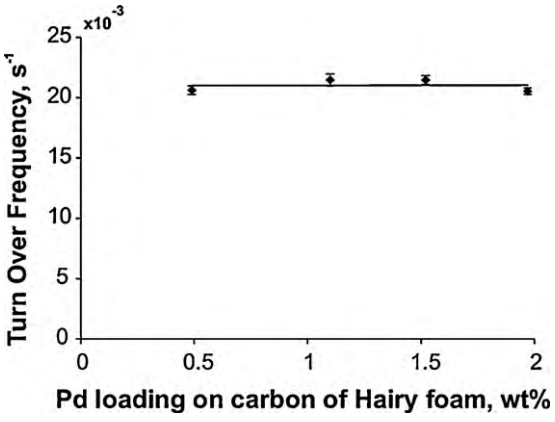

Fig. 9. Rate of nitrite conversion per mole of surface palladium on hairy foam catalysts at palladium loadings between 0.5 wt% and 2 wt% and a CNF-layer thickness of 13 μm measured at linear velocity of 55 cm/min and space velocity of 50.3 min^{-1}.

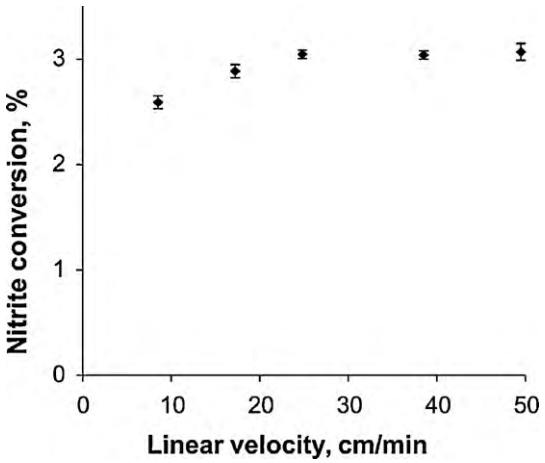

Fig. 10. Nitrite conversion as a function of linear velocity over 1.62 wt% Pd on activated carbon catalysts of 225 $_{avg}$ μm particle radius at a space velocity of 31.5 min^{-1}.

remaining constant at higher linear velocity. Further experiments with conventional catalysts were therefore performed using linear velocities larger than 25 cm/min, in order to avoid external mass transfer limitation.

Fig. 11 compares the TOF values as measured in fixed bed for palladium catalysts supported on alumina, activated carbon, graphite, silica as well as CNF aggregates. The properties of these catalysts are tabulated in Table 2. Fig. 11 demonstrates that smaller catalyst support particles are significantly more active as compared to larger catalyst particles for each specific support material. Furthermore, catalysts supported on CNF aggregates appear significantly more active than catalysts on conventional supports.

4. Discussion

4.1. Catalyst characterization

All conventional catalysts showed a reasonable homogenous distribution of Pd through the porous support (Fig. 5). The enhanced presence of Pd in the outer layer (Fig. 4) would make internal diffusion limitations less likely; however, this effect is probably compensated by the presence of Pd in the microporous carbon layer between the CNF-layer and the Ni foam surface [14], as Pd in the microporous layer would be less accessible. The result in Figs. 8 and 9 clearly demonstrates absence of any internal diffusion limitation, justifying the assumption that Pd is also homogenously distributed in hairy foam when discussing catalytic activity.

Pd particle sizes on hairy foams are all relatively large, between 11 nm and 20 nm, as reported in Table 3. Furthermore, the Pd dispersions of all catalysts are rather low, certainly when taking into

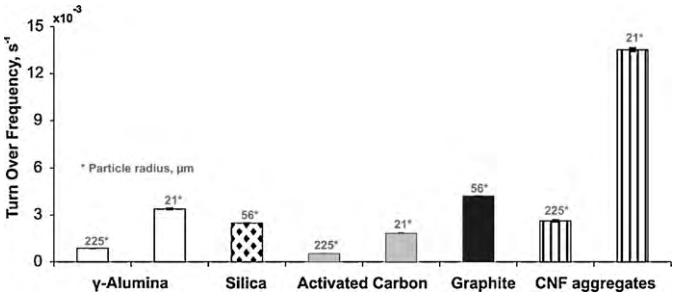

Fig. 11. Turn over frequency on catalysts such as, γ-alumina, activated carbon, unsupported CNF aggregates, silica and graphite at support particles radius of different radii.

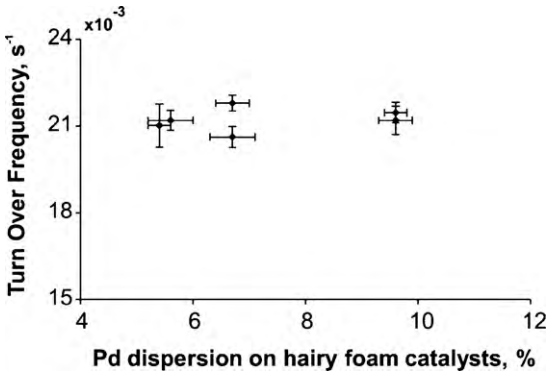

Fig. 12. Turn over frequency as a function of Pd dispersion for hairy foam catalysts.

consideration the low Pd loadings (0.5–2 wt%) used in this study. The reason for this is the choice to prepare the hairy foam catalysts on pristine CNFs, i.e. without prior oxidation of the CNFs, in order to prevent oxidative attack of the supporting Ni foam. As a consequence, the interaction between Pd particles and the CNFs is rather weak, contributing to low dispersions. All other catalysts were heat treated such that very similar dispersions were achieved (Table 3).

Mean particle sizes based on CO-chemisorption are clearly larger as compared to those based on TEM and XRD (Table 4). This difference might be due to uncertainty in the adsorption stoichiometry of CO-chemisorption on Pd [31] due to the preference to CO to bind to two or three Pd surface atoms instead of linear adsorption a single surface atom. Importantly, the large particle size according CO-chemisorption allows to rule out significant presence of very small particles (<2 nm), which is important because such particles are difficult to detect with TEM and are not detected at all with XRD. Thus, all techniques confirm that the differences in the particles sizes are modest and that the particles are generally large, which is an advantage in this study because significant support effects are unlikely. Larger particles are less prone to significant manipulation of the geometry or electronic structure of Pd by the support [22,32,33].

4.2. Catalyst activity

Hairy foam catalysts require higher linear velocities to overcome external mass transfer limitations as compared to a packed bed of catalyst supported on activated carbon (Fig. 7 *versus* Fig. 10). This can be understood in terms of the void space in the catalyst bed. The void fraction in hairy foam is much larger as compared to a packed bed, resulting in a lower actual velocity of the liquid as well as lower pressure drop. In other words, the shear forces, determining the thickness of the stagnant liquid layer at the external surface, are significant smaller as well. Therefore, hairy foam needs higher linear liquid velocity to prevent external mass transfer limitation.

The catalytic activity of hairy foam catalysts appears independent of the thickness of the CNF-layer and the Pd loading (Figs. 8 and 9). This demonstrates that internal mass transfer is not limiting and that the TOFs measured are indeed intrinsic. Fig. 12 shows that the TOFs is constant at around 0.021 s^{-1} for all hairy foam supported catalysts, despite modest variation of the Pd dispersion between 5% and 10%, confirming that the activity does not depend on Pd particle size for these relatively large particles. This value of TOF seems at first sight very small, but it should be noted that the concentrations of reactants in this study are extremely small. Our observations are in good agreement with Höller et al. [32], reporting similar TOFs for comparable Pd dispersions on γ-Al_2O_3 coated glass fibers. Fig. 11 shows that packed bed catalysts with small support particles (typ-

Table 5
Values of the Weisz–Prater parameter (C_{wp}) for different particles.

Support type	Radius of particle (μm)	C_{wp} values of reactants	
		NO_2^-	H_2
γ-Alumina	~225	5.08	6.56
γ-Alumina	~21	0.22	0.23
Activated carbon	~225	8.18	11.48
Activated carbon	~21	0.38	0.51
Silica	~56	0.32	0.37
Graphite	~56	3.48	5.13

ically 21 μm) are systematically more active as compared to large particles. This clearly suggests that large catalyst particles suffer from internal mass transfer limitations. This observation will now be further evaluated using the Weisz–Prater criterion as well as the Thiele modules. The details of the calculations as well as the diffusion coefficients used are described in the supporting information.

4.2.1. Estimation of internal mass transfer limitations via Weisz–Prater criterion (C_{WP})

Table 5 shows the results of the calculation of C_{wp} for all fixed bed catalysts, except the CNF aggregates. Unfortunately, no reliable data on the porosity of these materials are available. N_2 capillary-condensation results in an estimation of the pore volume of micropores and mesopores exclusively, resulting in typically 0.55 ml/g [29]. However, it should be noted that the morphology of entangled CNF particles and layers is very different compared to traditional porous catalyst support materials. The open volume is actually not contained in pores; in contrast the open volume is like a continuous phase and therefore adsorption and capillary-condensation methods fail. In any case, capillary-condensation is not able to determine the volume of macropores present in entangles CNF-structures. Jarrah et al. [6] estimated the pore volume of entangled CNF-layer on Ni foam at 1 ml/g, based on the thickness of the porous layer and its weight. In short, pore volumes based on N_2 capillary-condensation are resulting in significant underestimation. The C_{wp} values were calculated [34] for nitrite and hydrogen reactants involved in the reaction using values for pore volume and tortuosity as indicated in Table 2. C_{wp} values for protons were not calculated because of uncertainty about the H^+ or OH^- concentration to be used in the equation.

The C_{wp} values for all reactants and large catalyst particles (225 μm) are greater than 1, indicating that internal diffusion of both reactants is limiting, agreeing well with the observation that smaller particles are significantly more active. The C_{wp} values for small catalyst particles (21 μm and 56 μm, except for graphite) are below 1. Nevertheless, the values for nitrite and hydrogen indicate that internal mass transfer limitation may still influence the result to some extent. In order to estimate proton diffusion limitation and the significance of nitrite and hydrogen diffusion, efficiency factors have been estimated using the Thiele modules, using the intrinsic kinetic data obtained from hairy foam catalysts in this study.

4.2.2. Estimation of catalyst efficiency according the Thiele modulus ($ø_n$)

Assuming a first order reaction, maximal intrinsic rate constant ($k_{reactant}$) in this study was calculated from the reaction rate on hairy foam catalysts, in order to calculate Thiele moduli as well as effectiveness factors [34] for conventional catalysts, for each of the reactants. Table 6 presents the calculated Thiele moduli for alumina, activated carbon, silica and graphite catalysts with respective mean support particle radius. The large catalyst support particles (225 μm) show efficiency below 30% for nitrite and hydrogen, confirming a large influence of internal diffusion limitations, in agreement with experimental observations (Fig. 11) and calculations of the Weisz–Prater criterion. Smaller catalyst support particles (21 μm) as well as somewhat larger silica supported catalyst result in an efficiency of ~80–~90%. The limitation in protons is clearly less severe than in nitrite and hydrogen (Table 6), probably due to fast diffusion of protons. D'Arino et al. [23] suggested that proton diffusion is relatively slow as compared to diffusion of nitrite; this difference is due to the relatively low concentrations of nitrite and hydrogen in the present study. Thus, the catalytic activity of these small catalyst particles is only slightly affected by internal mass transfer limitation.

4.2.3. Comparison of catalysts

Fig. 13 compares the catalytic activity of the Pd catalysts with comparable diffusion-lengths, i.e. radius of particles and thickness of the active layer are similar for all catalysts. It is evident that the CNF based supports give much higher reaction rates. The advantage of CNF supports is also demonstrated in Fig. 11, by the fact that relatively large (225 μm) CNF aggregates result in much higher TOFs as compared to similar sized traditional support particles. Furthermore, the data in Figs. 8 and 9 convincingly demonstrate efficient mass transfer in CNF-layers up to 28 μm thick.

Enhanced mass transfer in CNF or CNT supported precious-metal catalysts in liquid phase reactions was also reported for hydrodehalogenation of bromobenzene [35], hydrogenation of *trans*-stilbene [36], cinnamaldehyde [37–39], citral [40] and nitrobenzene [41]. Increased activity is ascribed to better accessibility of active sites as compared traditional support materials.

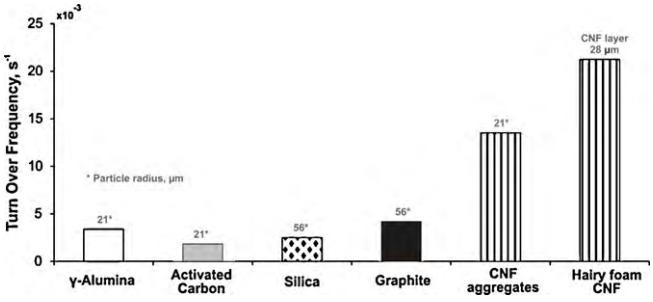

Fig. 13. Comparison of turn over frequency values of conventional catalysts and CNF based catalysts at comparable particle radius and CNF-layer thickness.

Table 6
Values of the Thiele modulus and effectiveness factor for different support particles.

Support type	Radius of Particle (μm)	Based on effective diffusivity of NO_2^-		Based on effective diffusivity of H_2		Based on effective diffusivity of H^+	
		Thiele modulus	Effectiveness factor	Thiele modulus	Effectiveness factor	Thiele modulus	Effectiveness factor
γ-Al_2O_3	~225	10.4	0.26	10.61	0.26	5.40	0.45
γ-Al_2O_3	~21	1.12	0.92	1.14	0.93	0.58	0.96
Activated carbon	~225	17.22	0.16	17.57	0.16	8.06	0.33
Activated carbon	~21	1.86	0.82	1.93	0.82	0.89	0.94
Silica	~56	1.49	0.88	1.52	0.87	0.78	0.97
Graphite	~56	4.02	0.56	4.10	0.55	2.10	0.75

However, possible influences of the support material on intrinsic activities of the mean particles were never systematically ruled out as in the present study.

Hydrogenation of nitrite is extremely fast, easily inducing internal concentration gradients due to diffusion limitation. Our results agree well with results of Strukul et al. [25], reporting that small catalyst support particles (diameter: 80 μm) are more active than large catalyst support particles (1.7 mm). However, our results demonstrate that 80 μm particles are still too large to prevent internal diffusion limitations. Lecloux [22] demonstrated that mass transfer limitations can be prevented using egg-shell catalysts with active metal located exclusively in the outer 20 μm of relatively large catalyst particles. Similarly, Hörold et al. [19] reported an increase in activity for nitrite reduction when increase the pore volume of alumina particles as small as 32 μm suggesting the influence of diffusion limitations.

We propose that both high porosity as well as low tortuosity of the CNF-layer contribute to the beneficial effect on activity. As discussed above, reliable experimental data on the porosity are lacking and the best information available so far is estimation from our lab (1 ml/g) based on microscopic estimation of thickness of the layer combined with weight of the carbon deposits [6]. However, Wenmakers [50] pointed out that the top layer of the CNF-layer is even more porous as compared to the bottom part of the CNF-layer. Given the fact that most Pd is deposited in the outer layer (Fig. 4), this might contribute to enhanced mass transfer. On the other hand, the morphology of layers of entangled CNF as observed on SEM directly hints to low tortuosity as compared to conventional catalyst supports.

Based on our observations and literature discussed above, we claim that CNF supports indeed provide better mass transfer properties; however, the high TOFs observed on CNF based supports cannot be due to mass transfer only. Based on the calculations of the WP number as well as Thiele number and the estimation of catalyst efficiency all indicate that catalysts supported on 21 μm radius particles of alumina and AC suffer only slightly from diffusion limitation. Therefore, the intrinsic activity of CNF-supported catalyst is significantly higher as compared to the other supports. The same effect is observed for graphite supported catalysts: despite internal diffusion limitations (Tables 5 and 6, due to the low porosity of graphite), the TOFs are relatively high. Therefore, the intrinsic activity of Pd on graphite must be significantly higher as compared to alumina, silica and activated carbon. These effects are certainly not artefacts due to differences in residence time distribution as all experiments are differential, keeping conversion below 6%. Further, Pd particle size and distributions are similar for all catalysts, whereas Fig. 12 demonstrates that TOF are constant within the window of variation of dispersion in this study as discussed above. In short, we rule out any particle size effects. Also, the Pd particles are too large to enable support materials to influence shape or electronic structure of the metal particles. Finally, conductivity of the support material is apparently not an important factor as AC supported catalyst are not particular active, in contrast to the CNF based supports as well as graphite.

Therefore, we speculate that the adsorption of reactants on the graphite support may also contribute to the activity. Nitrite possibly adsorbs directly on the graphite surface, inspired from [42,43] and/or hydrogen atoms spilled over from the Pd particles to the graphite surface [35,44] may contribute to the reaction rate at the perimeter of the catalyst particles. This is not uncommon in catalysis, for example for the liquid phase hydrogenation of cinnamaldehyde over Pt/CNF catalysts it was shown that catalytic action of Pt is influenced by the amount of cinnamaldehyde adsorbed on the support in the vicinity of Pt the particles [45,46]. Clearly, further research would be needed to clarify the underlying principle of this peculiar observation.

In short, hairy foams demonstrate advantages in terms of mass transfer, as well as intrinsic activity for nitrite hydrogenation under neutral conditions. Furthermore, hairy foams offer short diffusion paths without the disadvantage of high pressure drop in the case of a packed bed of small particles.

5. Conclusions

A series of Pd catalyst has been prepared with limited variation in Pd dispersion, containing relatively large (~10 nm) Pd particles, in order to study the effect of the morphology of the support material on the rate of internal mass transfer. It was demonstrated that the limited variation in Pd dispersions in this study indeed resulted in identical TOFs in nitrite hydrogenation for all hairy foam supported catalysts.

It was demonstrated that CNF based catalysts are indeed highly active for nitrite hydrogenation, resulting in TOFs at least three times larger as compared to conventional catalysts. This is due to improved mass transfer thanks to high porosity as well as low tortuosity of CNF aggregates as well as thin CNF-layers in hairy foam. Surprisingly, also the intrinsic activity of graphite and CNF-supported Pd contributes significantly to the high activity for nitrite reduction.

Hairy foam supports provide short diffusion pathways, combined with high porosity and low tortuosity, circumventing the disadvantage of small catalyst particles for liquid phase catalytic reactions, i.e. high pressure drop or the necessity of filtration.

Acknowledgements

This work was performed with the financial support from STW, Stichting voor de Technische Wetenschappen, Dutch funding organization (STW project # 6601). The authors greatly acknowledge RECEMAT for supplying Ni foam, we are grateful to Dr. M. Smithers for SEM, Dr. Enrico G. Keim for TEM, J.A.M. Vrielink for BET and XRF measurements, K. Altena-Schildkamp for CO-chemisorption measurements. We acknowledge Ing. B. Geerdink for technical support.

Appendix A. Supplementary data

Supplementary data associated with this article can be found, in the online version, at doi:10.1016/j.apcata.2010.05.013.

References

[1] A. Cybulski, J.A. Moulijn, Structured Catalysts and Reactors, second ed., Marcel Dekker, New York, 2006.
[2] T.A. Nijhuis, A.E.W. Beers, T. Vergunst, I. Hoek, F. Kapteijn, J.A. Moulijn, Catal. Rev. Sci. Eng. 43 (2001) 345–380.
[3] M.T. Kreutzer, F. Kapteijn, J.A. Moulijn, J.J. Heiszwolf, Chem. Eng. Sci. 60 (2005) 5895–5916.
[4] F. Kapteijn, J.J. Heiszwolf, T.A. Nijhuis, J.A. Moulijn, Cattech 3 (1999) 24–41.
[5] M.J. Ledoux, C. Pham-Huu, Catal. Today 102–103 (2005) 2–14.
[6] N. Jarrah, F. Li, J.G. van Ommen, L. Lefferts, J. Mater. Chem. 15 (2005) 1946–1953.
[7] A. Cordier, E. Flahaut, C. Viazzi, C. Laurent, A. Peigney, J. Mater. Chem. 15 (2005) 4041–4050.
[8] P.W.A.M. Wenmakers, J. van der Schaaf, F.M. Kuster, J.C. Schouten, J. Mater. Chem. 18 (2008) 2426–2436.
[9] P. Tribolet, L. Kiwi-Minsker, Catal. Today 103–103 (2005) 15–22.
[10] Z.R. Ismagilov, N.V. Shikina, V.N. Kruchinin, N.A. Rudina, A. Ushakov, N.T. Vasenin, H.J. Veringa, Catal. Today 102–103 (2005) 85–93.
[11] S.S. Tzeng, K.H. Hung, T.H. Ko, Carbon 44 (2006) 859–865.
[12] M. Cantoro, V.B. Golovko, S. Hofmann, D.R. Williams, C. Ducati, J. Geng, B.O. Boskovic, B. Kleinsorge, D.A. Jefferson, A.C. Ferrari, B.F.G. Johnson, J. Robertson, Diamond Relat. Mater. 14 (2005) 733–738.
[13] C. Stemmet. Gas–liquid solid foam reactors: hydrodynamics and mass transfer, PhD Thesis, Eindhoven University, 2008.
[14] J.K. Chinthaginjala, D.B. Thakur, K. Seshan, L. Lefferts, Carbon 46 (2008) 1638–1647.

[15] K.P. De Jong, J. Geus, Catal. Rev. Sci. Eng. 42 (2000) 481–510.
[16] P. Serp, M. Corrias, P. Kalck, Appl. Catal. A 253 (2003) 337–358.
[17] J.K. Chinthaginjala, K. Seshan, L. Lefferts, Ind. Eng. Chem. Res. 46 (2007) 3968–3978.
[18] N.M. Rodriguez, J. Mater. Res. 8 (1993) 3233–3250.
[19] S. Hörold, K.D. Vorlop, T. Tacke, M. Sell, Catal. Today 17 (1993) 21–30.
[20] S. Hörold, T. Tacke, K.D. Vorlop, Environ. Technol. 14 (1993) 931–939.
[21] A. Pintar, G. Bercic, J. Levec, AIChE 44 (1998) 2280–2292.
[22] A.J. Lecloux, Catal. Today 53 (1999) 23–34.
[23] M. D'Arino, F. Pinna, G. Strukul, Appl. Catal. B 53 (2004) 161–168.
[24] K.D. Vorlop, T. Tacke, Chem. Ing. Tech. 61 (1989) 836–837.
[25] G. Strukul, F. Pinna, M. Marella, L. Meregalli, M. Tomaselli, Catal. Today 27 (1996) 209–214.
[26] B. Gabel, R. Kozicki, U. Lahl, A. Podbielski, B. Stachel, S. Struss, Chemosphere 11 (1982) 1147–1154.
[27] C.G.M. van de Moesdijk, The catalytic reduction of nitrate and nitric oxide to hydroxylamine: kinetics and mechanism. Ph. D. Thesis, University of Eindhoven, 1979.
[28] J.K. Chinthaginjala, L. Lefferts, Carbon 47 (2009) 3175–3183.
[29] M.K. van der Lee, A.J. van Dillen, J.W. Geus, K.P. de Jong, J.H. Bitter, Carbon 44 (2006) 629–637.
[30] D.R. Lide, Handbook of chemistry and physics, 79th ed., CRC press, 1998.
[31] J.J.F. Scholten, A.P. Pijpers, A.M.L. Hustings, Catal. Rev. Sci. Eng. 27 (1985) 151–206.
[32] V. Höller, K. Rådevik, I. Yuranov, L. Kiwi-Minsker, A. Renken, Appl. Catal. B 32 (2001) 143–150.
[33] Y. Matatov-Meytal, Y. Shindler, M. Sheintuch, Appl. Catal. B 45 (2003) 127–134.
[34] H.S. Fogler, Elements of Chemical Reaction Engineering, third ed., Prentice-Hall Inc, 2002.
[35] L. Chen, A.C. Cooper, G.P. Pez, H. Cheng, J. Phys. Chem. C 111 (2007) 18995–19000.
[36] T. Onoe, S. Iwamoto, M. Inoue, Catal. Commun. 8 (2007) 701–706.
[37] C. Pham-Huu, N. Keller, G. Ehret, L. Charbonniere, R. Ziessel, M.J. Ledoux, J. Mol. Catal. A 170 (2001) 155–163.
[38] J. Tessonnier, L. Pesant, G. Ehret, M.J. Ledoux, C. Pham-Huu, Appl. Catal. A 288 (2005) 203–210.
[39] H. Vu, F. Goncalves, R. Philippe, E. Lamouroux, M. Corrias, Y. Kihn, D. Plee, P. Kalck, P. Serp, J. Catal. 240 (2006) 18–22.
[40] F. Qin, W. Shen, C. Wang, H. Xu, Catal. Commun. 9 (2008) 2095–2098.
[41] C. Li, Z. Yu, K. Yao, S. Ji, J. Liang, J. Mol. Catal. A 226 (2005) 101–105.
[42] S.D. Ebbesen, B.L. Mojet, L. Lefferts, Langmuir 24 (2008) 869–879.
[43] A. Miyazaki, T. Asakawa, I. Balint, Appl. Catal. A 363 (2009) 81–85.
[44] D.J. Browning, M.L. Gerrard, J.B. Lakeman, I.M. Mellor, R.J. Mortimer, M.C. Turpin, Nano Lett. 2 (2002) 2001–2005.
[45] M.L. Toebes, T.A. Nijhuis, J. Hájek, J.H. Bitter, A.J. van Dillen, D.Yu. Murzin, K.P. de Jong, Chem. Eng. Sci. 60 (2005) 5682–5695.
[46] A.J. Plomp, H. Vuori, A.O.I. Krause, K.P. de Jong, J.H. Bitter, Appl. Catal. A 351 (2008) 9–15.
[47] K.C. Metaxas, N.G. Papayannakos, Chem. Eng. J. 140 (2008) 352–357.
[48] R. Leyva-Ramos, C.J. Geankoplis, Can. J. Chem. Eng. 72 (1994) 262–271.
[49] W. Xia, C. Jin, S. Kundu, M. Muhler, Carbon 47 (2009) 919–922.
[50] P.W.A.M. Wenmakers. Hairy foam: carbon nanofibers on solid foam as catalyst support, PhD Thesis, Eindhoven University, 2010.